Terahertz wave transmission in flexible polystyrene-lined hollow metallic waveguides for the 2.5-5 THz band

Miguel Navarro-Cía,[1,2] Miriam S. Vitiello,[3] Carlos M. Bledt,[4,5] Jeffrey E. Melzer,[4] James A. Harrington,[4] and Oleg Mitrofanov[1,*]

[1]*Department of Electronic and Electrical Engineering, University College London, London WC1E 7JE UK*
[2]*Currently with the Optical and Semiconductor Devices Group, Department of Electrical and Electronic Engineering, Imperial College London, London SW7 2BT, UK and the Centre for Terahertz Science and Engineering, Imperial College London, London SW7 2AZ, UK*
[3]*NEST, CNR—Istituto Nanoscienze and Scuola Normale Superiore, Pisa, Italy*
[4]*School of Engineering, Rutgers University, 607 Taylor Road, Piscataway, New Jersey 08854 USA*
[5]*School of Engineering, Brown University, 182 Hope Street, Providence, Rhode Island 02912 USA*
[*]*o.mitrofanov@ucl.ac.uk*

Abstract: A low-loss and low-dispersive optical-fiber-like hybrid HE_{11} mode is developed within a wide band in metallic hollow waveguides if their inner walls are coated with a thin dielectric layer. We investigate terahertz (THz) transmission losses from 0.5 to 5.5 THz and bending losses at 2.85 THz in a polystyrene-lined silver waveguides with core diameters small enough (1 mm) to minimize the number of undesired modes and to make the waveguide flexible, while keeping the transmission loss of the HE_{11} mode low. The experimentally measured loss is below 10 dB/m for $2 < \nu < 2.85$ THz (~4-4.5 dB/m at 2.85 THz) and it is estimated to be below 3 dB/m for $3 < \nu < 5$ THz according to the numerical calculations. At ~1.25 THz, the waveguide shows an absorption peak of ~75 dB/m related to the transition between the TM_{11}-like mode and the HE_{11} mode. Numerical modeling reproduces the measured absorption spectrum but underestimates the losses at the absorption peak, suggesting imperfections in the waveguide walls and that the losses can be reduced further.

OCIS codes: (110.6795) Terahertz imaging; (140.5965) Semiconductor lasers, quantum cascade; (180.4243) Near-field microscopy; (300.6495) Spectroscopy, terahertz; (320.7100) Ultrafast measurements.

References and links

1. P. G. Gallot, S. P. Jamison, R. W. McGowan, and D. Grischkowsky, "Terahertz waveguides," J. Opt. Soc. Am. B **17**(5), 851–863 (2000).
2. H. Han, H. Park, M. Cho, and J. Kim, "Terahertz pulse propagation in a plastic photonic crystal fiber," Appl. Phys. Lett. **80**(15), 2634–2636 (2002), http://apl.aip.org/resource/1/applab/v80/i15/p2634_s1.
3. K. Nielsen, H. K. Rasmussen, A. J. Adam, P. C. Planken, O. Bang, and P. U. Jepsen, "Bendable, low-loss Topas fibers for the terahertz frequency range," Opt. Express **17**(10), 8592–8601 (2009).
4. A. Dupuis, J.-F. Allard, D. Morris, K. Stoeffler, C. Dubois, and M. Skorobogatiy, "Fabrication and THz loss measurements of porous subwavelength fibers using a directional coupler method," Opt. Express **17**(10), 8012–8028 (2009).
5. Y. Matsuura and E. Takeda, "Hollow optical fibers loaded with an inner dielectric film for terahertz broadband spectroscopy," J. Opt. Soc. Am. B **25**(12), 1949–1954 (2008), http://www.opticsinfobase.org/josab/abstract.cfm?uri=josab-25-12-1949.
6. A. L. Bingham and D. R. Grischkowsky, "Terahertz 2-D photonic crystal waveguides," IEEE Microw. Wirel. Comp. Lett. **18**, 428–430 (2008). *http://ieeexplore.ieee.org/xpl/articleDetails.jsp?arnumber=4536885*
7. R. Mendis and D. M. Mittleman, "Comparison of the lowest-order transverse-electric (TE_1) and transverse-magnetic (TEM) modes of the parallel-plate waveguide for terahertz pulse applications," Opt. Express **17**(17), 14839–14850 (2009).
8. O. Mitrofanov, R. James, F. Aníbal Fernández, T. K. Mavrogordatos, and J. A. Harrington, "Reducing transmission losses in hollow THz waveguides," IEEE Trans. THz Sci. Tech. (Paris) **1**, 124–132 (2011), http://ieeexplore.ieee.org/xpl/articleDetails.jsp?arnumber=6005337.

#190912 - $15.00 USD Received 21 May 2013; revised 20 Aug 2013; accepted 22 Aug 2013; published 30 Sep 2013

9. O. Mitrofanov and J. A. Harrington, "Dielectric-lined cylindrical metallic THz waveguides: mode structure and dispersion," Opt. Express **18**(3), 1898–1903 (2010).
10. B. Bowden, J. A. Harrington, and O. Mitrofanov, "Low-loss modes in hollow metallic terahertz waveguides with dielectric coatings," Appl. Phys. Lett. **93**(18), 181104 (2008), http://apl.aip.org/resource/1/applab/v93/i18/p181104_s1.
11. X.-L. Tang, Y.-W. Shi, Y. Matsuura, K. Iwai, and M. Miyagi, "Transmission characteristics of terahertz hollow fiber with an absorptive dielectric inner-coating film," Opt. Lett. **34**(14), 2231–2233 (2009).
12. M. Miyagi and S. Kawakami, "Design theory of dielectric-coated circular metallic waveguides for infrared transmission," J. Lightwave Technol. **2**(2), 116–126 (1984), http://ieeexplore.ieee.org/xpls/abs_all.jsp?arnumber=1073590.
13. J. A. Harrington, *Infrared Fiber Optics and Their Applications* (SPIE, 2004).
14. C. M. Bledt, J. E. Melzer, and J. A. Harrington, "Fabrication and characterization of improved Ag/PS hollow glass waveguides for THz transmission," Submitted to Applied Optics (May 2013).
15. O. Mitrofanov, T. Tan, P. R. Mark, B. Bowden, and J. A. Harrington, "Waveguide mode imaging and dispersion analysis with terahertz near-field microscopy," Appl. Phys. Lett. **94**(17), 171104 (2009), http://apl.aip.org/resource/1/applab/v94/i17/p171104_s1.
16. M. Navarro-Cía, C. M. Bledt, M. S. Vitiello, H. E. Beere, D. A. Ritchie, J. A. Harrington, and O. Mitrofanov, "Modes in AgI lined hollow metallic waveguides mapped by terahertz near-field time-domain microscopy," J. Opt. Soc. Am. B **30**(1), 127–135 (2013).
17. M. S. Vitiello, J.-H. Xu, F. Beltram, A. Tredicucci, O. Mitrofanov, J. Harrington, H. E. Beere, and D. A. Ritchie, "Guiding a terahertz quantum cascade laser into a flexible silver-coated waveguide," J. Appl. Phys. **110**, 063112 (2011), http://jap.aip.org/resource/1/japiau/v110/i6/p063112_s1.
18. M. S. Vitiello, G. Scamarcio, V. Spagnolo, S. S. Dhillon, and C. Sirtori, "Terahertz quantum cascade lasers with large wall-plug efficiency," Appl. Phys. Lett. **90**(19), 191115 (2007), http://apl.aip.org/resource/1/applab/v90/i19/p191115_s1.
19. http://spectra.iao.ru/en/en/home/
20. P. Doradla, C. S. Joseph, J. Kumar, and R. H. Giles, "Characterization of bending loss in hollow flexible terahertz waveguides," Opt. Express **20**(17), 19176–19184 (2012).
21. V. Setti, L. Vincetti, and A. Argyros, "Flexible tube lattice fibers for terahertz applications," Opt. Express **21**(3), 3388–3399 (2013).
22. J. R. Birch, "The far-infrared optical constants of polypropylene, PTFE, and polystyrene," Infrared Phys. **33**(1), 33–38 (1992), http://www.sciencedirect.com/science/article/pii/002008919290052U.

1. Introduction

Transmission of terahertz (THz) waves has been predominantly realized as free-space beams propagating in air to avoid relatively strong absorption in most media in the THz range. However, even air causes absorption and dispersion, particularly in the region above 1 THz. Recently, THz waveguides have been shown to allow transmitting THz waves with losses comparable to absorption in air [1–7]. It is achieved through engineering the dominant mode of the waveguide to minimize distribution of the transmitted wave in the material (metal or dielectric) [7,8]. Among recently demonstrated low-loss THz waveguides [8] are the dielectric-lined waveguides that support the linearly polarized HE_{11} mode as the dominant mode of propagation [9]. This mode can have low attenuation, as low as 1 dB/m for a 2.2 mm diameter waveguide [10], and low dispersion of 6 ps/THz/m at ~2 THz [9]. The closed walls in this hollow waveguide allow filling the waveguide volume with nitrogen gas or dry air to avoid absorption due to water vapor.

Dispersion and attenuation properties in this waveguide critically depend on the dielectric layer properties and the waveguide diameter [11–13]. The thickness of the dielectric layer determines the spectral position of the transmission band. A dielectric layer thickness of the order of 10-20 μm is required for the THz band when using common polymers with refractive indices ranging from 1.5 to 2. Meanwhile, the waveguide diameter affects the loss and dispersion properties. The loss is inversely proportional to the third power of the diameter [13]. Although the loss can be minimized by increasing the waveguide diameter, waveguide flexibility for large diameters reduces and the number of undesired modes increases. Flexible waveguides have been recently fabricated using small diameter (~1 mm) glass tubes coated with silver and polystyrene (PS) layers and the quality of the PS film investigated at mid-infrared wavelengths [14]. The small diameter permits bending this waveguide to a radius of 100-150 mm [Fig. 1(a) and inset of Fig. 1(b)] and it is expected that they support the HE_{11} mode at THz frequencies.

#190912 - $15.00 USD Received 21 May 2013; revised 20 Aug 2013; accepted 22 Aug 2013; published 30 Sep 2013

In this paper we characterize the spectral properties of the 1 mm-diameter PS-lined waveguides at THz frequencies. We perform broadband cutback loss measurement using a near-field time-domain spectroscopy (TDS) system for the low frequency absorption band and for the low-frequency part of the transmission band (ν = 0.5 – 2.5 THz, i.e., λ = 120 – 600 μm). This approach mitigates the characterization difficulties associated to mode interference, pulse dispersion and large variation of the coupling coefficient and loss with frequency. We also show high precision single-frequency cutback loss and bending loss measurements for ν = 2.85 THz within the transmission band using a quantum cascade laser (QCL). Finally, we provide numerical calculations of the transmission loss spectra and mode profile evolution from 0.5 to 5.5 THz to understand the origin of the loss variation and estimate the transmission losses for the frequency range not covered experimentally. The experimental near-field TDS data shows the formation of the low-loss transmission band in the 1 mm diameter PS-lined hollow waveguide. The band spans ~2.5 THz, from 2.5 to 5 THz, as confirmed by numerical modeling. The waveguide shows the absorption of ~4-4.5 dB/m within the transmission band, matching the calculated loss level. The experimentally measured spectrum however shows a much higher absorption level (~75 dB/m) within the absorption band (at ~1.2 THz). We demonstrate that the absorption band is caused by the change in the profile of the dominant hybrid mode, which may affect the loss within the transmission band. In the absorption band center the mode profiles show local maxima at the metallic walls. The experimental results therefore potentially indicate the impact that the metallic layer has on the waveguide performance. The difficulty of explaining experimental data with standard numerical models of surface roughness suggests that it needs to be addressed more rigorously.

The position of the transmission band with relatively low transmission losses, the flexibility and reduced diameter make these waveguides viable for applications with THz QCL sources, for instance, endoscopic applications [13].

2. Experiments, modeling and discussion

The PS-lined hollow metallic waveguide under study here consists of a 1 mm bore diameter fused silica capillary tube with a ~0.6 μm thick Ag film on the internal face and additional 10 ± 1 μm thick PS inner coating [14]. Details of the fabrication can be found in Ref. 14. The dielectric layer on the inner wall of the waveguide is designed to alter the transmission spectrum and form a transmission band in the THz region, in which the waveguide loss decreases to ~2-5 dB/m for the hybrid HE_{11} mode. The reduced loss within the transmission band is due to the mode profile of the HE_{11} mode, in which the electric field amplitude decreases to zero along the entire circumference of the waveguide wall. Outside the transmission band, waveguide absorption increases to a level over 20 dB/m due to changes in the hybrid mode profile. The experiments discussed below are designed to verify the predicted behavior [14].

The near-field mode spectroscopy and imaging system for waveguide characterization [15] is shown in Fig. 1(b)-1(c). A 1 mm thick ZnTe crystal is used for generation of THz pulses by optical rectification of 100 fs pulses from a Ti:Sapphire mode-locked laser. The THz beam is collimated by a 3 mm diameter hyper hemispherical lens (SL) with the waveguide samples being positioned at a distance of ~500 μm away from the lens. In order to improve coupling of the incident THz beam to the dominant waveguide mode (HE_{11}), a metallic screen with a 600 μm pinhole (P) is placed between the lens and the waveguide input. The pinhole reduces coupling of the incident wave to the HE_{12} mode (as observed in the amplitude of periodic structure of the transmitted pulse spectrum in comparison to excitation without the pinhole). The output of the waveguide is positioned in front of the integrated THz near-field probe (NFP), as shown in Fig. 1(c). The probe contains a LT GaAs photoconductive detector and a 10 μm × 10 μm sub-wavelength aperture, which allows mapping the electric field distribution in the waveguide output plane. Although the detected signal is reduced by low transmission through the small aperture, the probe allows probing and mapping the electric field of the propagating wave without introducing effects of the THz

#190912 - $15.00 USD Received 21 May 2013; revised 20 Aug 2013; accepted 22 Aug 2013; published 30 Sep 2013

wave coupling to the photoconductive antenna. The probe senses the horizontal polarization, E_x, of the incoming THz wave. The waveguide is enclosed into a sealed holder and purged with N_2 to remove absorption to water vapor.

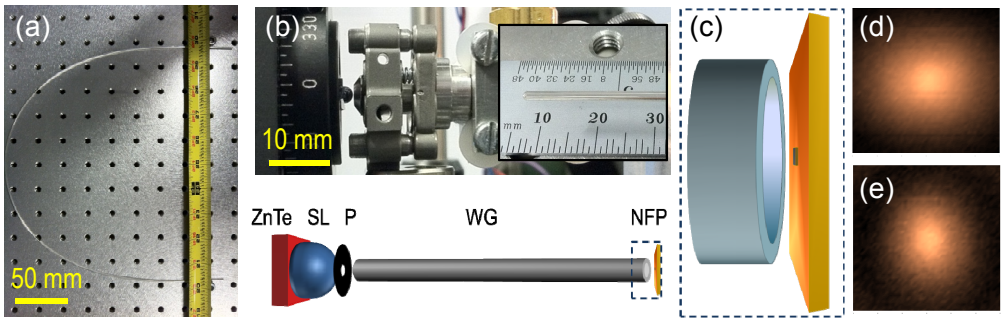

Fig. 1. (a) Photograph of the PS-lined cylindrical metallic waveguide. (b) Photograph of the input section (top) and schematic of the near-field waveguide mode imaging system (bottom). Inset: detail of the PS-lined cylindrical metallic waveguide. (c) Schematic of the sub-wavelength aperture near-field probe configuration. Near-field electric field E_x profiles (1.2 mm × 1.2 mm) at the output of the cylindrical metallic waveguide without (d) and with (e) the PS internal layer showing the TE_{11} and HE_{11} modes.

Short waveguide samples of 80 and 300 mm in length are used to determine transmission properties in the range from 0.5 to 2.5 THz with the 80 mm waveguide segment being used as a launch waveguide. The hybrid HE_{11} mode develops at the output of the launch waveguide, as can be seen in a near-field electric field map of the mode at the peak of the transmitted pulse. The map presented in Fig. 1(e) shows the expected hybrid mode profile. It is noticeably different from the profile of the classical TE_{11} mode in a similar silver hollow waveguide without the PS coating [Fig. 1(d)]. The 300 mm long waveguide segment is then measured to determine transmission losses caused by the additional 220 mm of the waveguide. The length of 300 mm is chosen to yield measurable loss levels within both the transmission and absorption spectral regions.

The waveforms detected on the waveguides axis for both lengths are shown in Fig. 2. Apart from the waveguide-induced dispersion, the 80 mm segment waveform indicates the presence of the HE_{12} mode at t = 12-15 ps, whose amplitude is not completely negligible as it happens with higher order modes. This HE_{12} mode is less noticeable in the 300 mm segment waveform (t ~30 ps). The leading section of the pulse [Fig. 2(b) inset] in fact shows only the HE_{11} mode. The waveguide transmission spectrum is found by taking a ratio of the measured waveform spectra [Fig. 3(a), 3(b)]. The measured frequency range covers both the low-frequency absorption band and a large portion of the transmission band [8,14]. The rapid oscillations observed in both waveform spectra on top of a base line, which is associated to the HE_{11} mode, accounts for the presence of the HE_{12} mode [Fig. 3(a)].

In the transmission band, losses decrease to a level of ~5 dB/m at approximately 2.5 THz. The experimental spectrum is consistent with the prediction that transmission loss is minimal for this waveguide at ~3-4 THz [14]. The small amount of power output at frequencies above 2.5 THz in the TDS system however does not allow us to characterize transmission in this frequency range. The low level of absorption in this band also makes the measurement susceptible to experimental errors due to the presence of higher order modes, which cause periodic ripples in the spectra of the transmitted pulses [Fig. 3(a)], and due to possible system misalignment during interchanging waveguide samples.

#190912 - $15.00 USD Received 21 May 2013; revised 20 Aug 2013; accepted 22 Aug 2013; published 30 Sep 2013

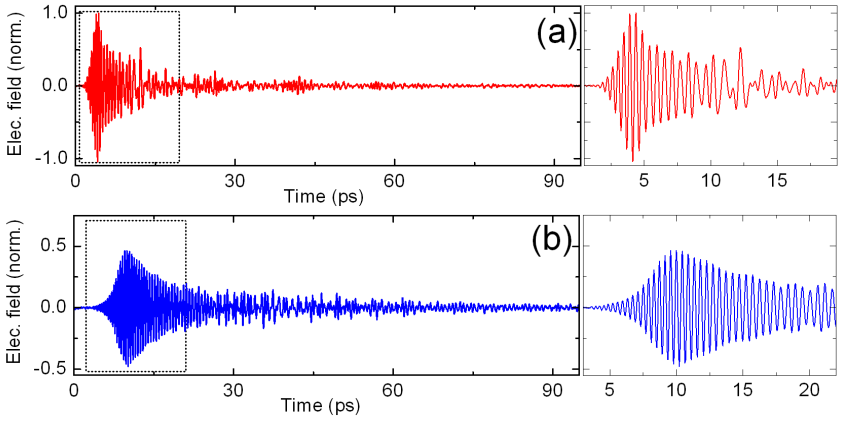

Fig. 2. Waveforms detected on the waveguide axis after propagating through an 80 mm long (a) and 300 mm long (b) Ag/PS waveguide.

From about 1 to 1.5 THz, there is an absorption band within which the transmission loss increases to 70–80 dB/m. This band is caused by the change in the hybrid mode spatial profile. To track this change, the numerically-computed total electric field distribution, $20\log_{10}|E(x,y)|$, (details of the modeling are given in the appendix) is shown in Fig. 3(c) for different frequencies. From this set of color maps one can notice that a significant portion of the mode energy is shifted to the waveguide walls in the absorption band, resembling the TM_{11} mode of uncoated cylindrical hollow metallic waveguides. Both the dielectric loss and Ohmic losses contribute to the waveguide absorption within this band.

To verify the performance of the Ag/PS hollow waveguides, we estimate numerically the transmission loss for $\nu > 2.85$ THz and illustrate the effects of the dielectric and metal layers using different combinations of silver conductivity, PS loss tangent ($\tan\delta = \mathrm{Re}(\varepsilon)/\mathrm{Im}(\varepsilon)$) and dielectric thickness [Fig. 3(b), 3(c)]. For ideal conditions, σ_{Ag} and $\tan\delta = 0.005$ (blue dotted line), the simulated loss ranges from 1.95 dB/m at 3.0 THz and to 22.08 dB/m at 1.2 THz. When the dielectric loss is increased to $\tan\delta = 0.023$ (black dash-dot line), both inflection points rise to 5.03 and 54.04 dB/m, respectively. When an intermediate value of dielectric loss ($\tan\delta = 0.010$) and the effective conductivity of silver ($0.32\sigma_{Ag}$) are considered (blue dashed line), these characteristics points are 3.28 and 41.71 dB/m, respectively. This analysis underlines the strong dependence of the attenuation on the material properties at the absorption band given the significant shift of mode energy to the waveguide walls.

The experimental spectrum shows similar behavior, however the experimental loss in the absorption band is substantially higher. The origin of this loss is likely to be the surface roughness of the metallic layer, which may cause non-perfect contact between the silver and the PS coating [5,13]. This effect is not modeled by the effective conductivity and it is rather complex to be modeled numerically.

In Fig. 3(c) one can see the direct proportionality between the frequency band and the dielectric thickness following the analytical relation [12,13]:

$$\lambda_d = d \cdot 2\pi\sqrt{n_d^2 - 1} \cdot \tan\left(\frac{n_d}{\left(n_d^2 - 1\right)^{1/4}}\right) \qquad (1)$$

where λ_d is the design wavelength, d the PS thickness and n_d is the real part of the refractive index of PS at λ_d. A thicker coating red-shifts the absorption and transmission bands. For instance, the 14 μm PS coating produces the first transmission band from 2 to 4 THz, and the low-frequency end of the second transmission band for this PS coating starts at around 5 THz. Meanwhile, the 8 μm PS coating produces the first transmission band that starts slightly blue-shifted with respect to the 10 μm PS coating, and its high-frequency end is beyond the

#190912 - $15.00 USD Received 21 May 2013; revised 20 Aug 2013; accepted 22 Aug 2013; published 30 Sep 2013

spectral window shown. On the other hand, there exists also a relation between *d* and transmission losses. In a first approximation, the attenuation of the HE_{11} mode can be expressed as a sum of the attenuation constant of the HE_{11} mode without the dielectric absorption (α_{HE11}) and additional loss due to absorption in the PS-coating (α_{PS}), which is proportional to the dielectric thickness [5]. The data from Fig. 3(c) indicate this for λ_d: the minimum loss for 8, 10 and 14 μm thick PS inner coating (with σ_{Ag} and tan δ = 0.005) is 0.64, 0.96 and 1.88 dB/m, respectively.

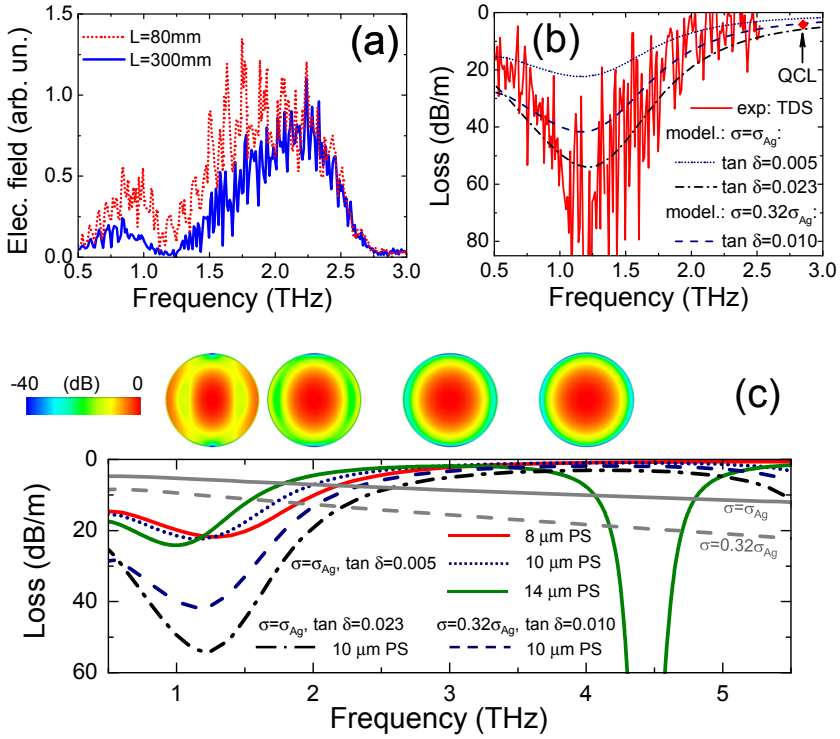

Fig. 3. (a) Spectra corresponding to the waveforms of Fig. 2. (b) Experimental and modeled transmission loss spectra of the Ag/PS waveguide. The diamond shows the experimentally measured transmission loss of ~4.2 dB/m using a single frequency (2.85 THz) QCL and the cutback method. (c) Modeled transmission loss spectra up to 5.5 THz of the Ag-only waveguide with σ_{Ag} (solid gray line) and $\sigma = 0.32\sigma_{Ag}$ (dashed gray line), and of the Ag/PS waveguide with PS thickness: 8 μm (red line), 10 μm (colors and line styles as panel (b)) and 14 μm (green line). Top insets: amplitude of the field distribution in dB for 10 μm PS coating at notable frequencies; from left to right: 1.2, 2, 3 and 4 THz.

The THz pulse transmission in the 80 mm long Ag/PS waveguide is also compared to that in an 80 mm long waveguide without the PS coating, whose fundamental mode is the TE_{11} mode. The hollow silver-coated waveguide exhibits no absorption band at 1.2 THz. It has a featureless transmission spectrum within the characterized region (from 0.5 THz to 2.5 THz) with the loss increasing practically linearly [16]. By comparing the numerically-computed transmission loss spectra of the Ag-only waveguide [gray lines in Fig. 3(c)] with that of any of the previous Ag/PS simulated cases, we notice that transmission losses above ~2 THz are lower in the Ag/PS waveguides compared to the Ag-only waveguides. The inflection point corresponds to the onset of the optical-fiber-like HE_{11} mode. At the transmission band center, the PS coating brings an improvement of ~10 dB/m compared to the ideal Ag-only waveguide and ~17 dB/m when the effective conductivity of silver ($0.32\sigma_{Ag}$) is considered. Within the absorption band 1-1.5 THz, however, the loss level in the Ag/PS waveguides is considerably higher and it is consistent with the measurements on the 80 mm and 300 mm Ag/PS samples.

#190912 - $15.00 USD Received 21 May 2013; revised 20 Aug 2013; accepted 22 Aug 2013; published 30 Sep 2013

For more precise waveguide characterization in the transmission band, single frequency cutback measurements on longer samples (up to 1 m) are performed [17]. A 2.85 THz QCL is mounted on the cold finger of a continuous-flow liquid-helium cryostat and driven with 200 ns pulses at 10 kHz repetition rate at a current of 0.8A [18]. The QCL beam is coupled into the hollow waveguide with a 3 cm focal length Picarin lens, which focuses the laser beam into $a \approx 1$ mm spot [17] at the waveguide input. A pinhole in thin stainless steel is positioned in contact with the waveguide input. The pinhole diameter is kept identical to the waveguide hollow core. A calibrated pyroelectric detector, having a sensitive area of about 3 mm, is mounted on a XY translational stage, driven by stepper motors with a spatial resolution of 0.2 μm to scan across the waveguide output and image the mode profile at the output (~2 cm from the waveguide). The detected power at each scanning position is therefore recorded in the far-field of the waveguide output. Figure 4(a) shows the far field spatial intensity distribution of the QCL, upon exiting a 60 mm long waveguide measured while focusing the vertically polarized QCL beam directly at the center of the hollow waveguide axis. By centering the position of the input beam on the waveguide axis the launched TE_{11} laser mode [18], after propagation through the waveguide, fully develops as a HE_{11} mode at the output as shown from the measured far-field profile of Fig. 4(a). The measured loss for the Ag/PS waveguide at 2.85 THz in air sample is approximately 4.7 dB/m. Taking into consideration that at 2.85 THz the typical loss of air is approximately > 0.5 dB/m [19], the loss due to the actual PS-lined hollow waveguide can be approximated to be at most ~4.2 dB/m.

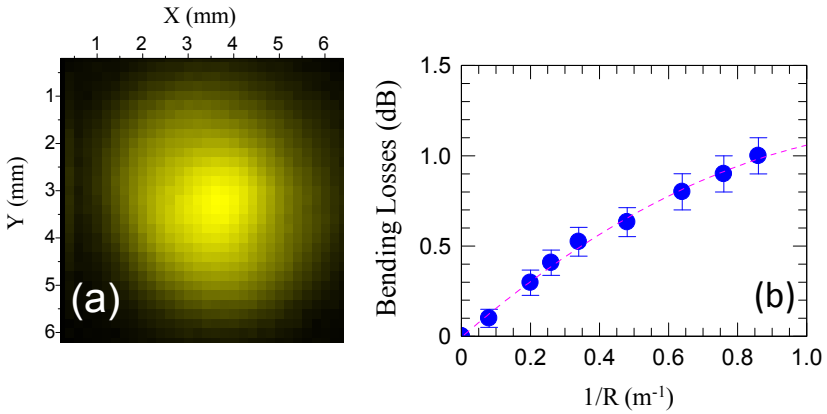

Fig. 4. (a) Far field spatial intensity distribution of a 2.85 THz QCL upon exiting a 1 m long, 1 mm bore diameter Ag/PS flexible hollow waveguide. The beam profile has been measured by focusing the QCL beam directly at the center of hollow waveguide axis by means of an f/1 Picarin lens. (b) Bending losses for a 1 m long waveguide measured while coupling the QCL with a 3 cm focal length Picarin. The dashed line is a quadratic fit to the data. The error bars show absolute errors for each individual data point calculated using the standard deviation in the power measurements.

To measure the waveguide bending losses, the center part of the tube is bent in a uniform curvature keeping the polarization of the incoming THz beam perpendicular to the plane of bending. This condition should give in principle lower losses than the polarization parallel to the bending plane. The measured losses increase as the curvature increases, reaching 1.0 dB/m at the bending angle of 45°, corresponding to the radius of curvature of 1.25 m [Fig. 4(b)]. It is worth mentioning that the dominant HE_{11} mode remains practically unperturbed by the waveguide bending given the reduced size of the bore diameter and large bending radii [20]. Hence, the bending losses follow a quadratic ($1/R^2$) law. We note that for smaller bending radii the quadratic relation may break down [21].

3. Conclusions

Flexible polystyrene-lined hollow metallic waveguides of bore diameter 1 mm designed for the 2.5-5THz band are analyzed experimentally and numerically. Transmission properties of

#190912 - $15.00 USD Received 21 May 2013; revised 20 Aug 2013; accepted 22 Aug 2013; published 30 Sep 2013

the hybrid HE_{11} mode are measured experimentally, despite the multimode nature of this waveguide. Within the transmission band (2.5 – 5 THz), absorption drops to a value below 5 dB/m. Bending loss below 1 dB/m is measured for bending radii down to 1.25 m. At lower frequencies, the absorption increases up to ~75 dB/m (in the range 0.5 – 1.25 THz) and then recovers to ~15 dB/m. This behavior is explained by the change in the field profile from the hybrid HE_{11} mode at higher frequencies to a TM_{11}-like mode at low frequencies. The strong attenuation within the absorption band is substantially higher than our numerical estimations. Although the increased loss is observed mainly in the absorption band, the 'tail' of the absorption band affects the waveguide performance at the lower frequency side of the transmission band. It suggests that the waveguide walls quality plays an important role, which so far has not been addressed for these waveguides, and the transmission loss figures for this waveguide may be improved to the level of 2 dB/m.

Appendix: Numerical simulations

The transmission properties of the PS-lined cylindrical waveguide are modeled with CST Microwave Studio™ using a 2-D eigenmode analysis [16]. To simplify the calculation, the silica tubing is not considered in the waveguide system. This is a reasonable approximation since the thickness of the silver film is much larger than the skin depth of silver in the spectral region of interest. The simulated geometry consists of a lossy silver film and a 10 μm thick PS film around a 1 mm diameter loss-free air core. Two different conductivities are considered for the silver layer: the bulk silver conductivity $\sigma_{Ag} = 6.3012 \times 10^7$ S/m and a reduced conductivity, $\sigma = 0.32\sigma_{Ag}$. The latter is an effective conductivity computed through the Hammerstad-Jensen approach that takes into account the roughness of the metal. The dielectric property of the PS is based on tabulated experimental data [22]. The relative permittivity is assumed constant $\varepsilon_r = 2.49$ and the loss tangent $\tan\delta = \mathrm{Re}(\varepsilon)/\mathrm{Im}(\varepsilon) = 0.005$. Additionally, higher dielectric losses are studied with $\tan\delta = 0.010$ and 0.023 to account for potential fabrication issues and to show the effect of this parameter in the loss spectrum. For comparison purposes, the same cylindrical waveguide without the dielectric coating is also calculated. Given the twofold symmetry of the problem, a vertical electric and a horizontal magnetic mirror planes have been applied to consider only a quarter of the waveguide cross section. An adaptive tetrahedral discretization with maximum edge length of 5.5 μm within the waveguide circumference is used to match accurately the circular cross-sectional area of the waveguide.

Acknowledgments

M.N.-C. is supported by Imperial College London through a Junior Research Fellowship. M.S.V. acknowledges financial support of the Italian Ministry of Education, University, and Research (MIUR) through the program "FIRB-Futuro in Ricerca 2010" RBFR10LULP "Fundamental research on terahertz photonic devices". This work was also supported by the Engineering and Physical Sciences Research Council (grant numbers EP/G033870/1 and EP/J017671/1), the Royal Society (grant number UF080745).

#190912 - $15.00 USD Received 21 May 2013; revised 20 Aug 2013; accepted 22 Aug 2013; published 30 Sep 2013